J Fluoresc (2016) 26:1497–1504
DOI 10.1007/s10895-016-1847-7

ORIGINAL ARTICLE

Multi-Color Luminescence and Sensing of Rare Earth Hybrids by Ionic Exchange Modification

Han Weng[1] · **Bing Yan**[1]

Received: 13 February 2016 / Accepted: 30 May 2016 / Published online: 15 June 2016

Abstract Luminescent rare earth coordination polymers $[H_2NMe_2]_3[Y(DPA)_3]$ ($[H_2NMe_2]^+$ = dimethyl amino cation; H_2DPA = 2,6-dipicolinic acid) are synthesized and is further modified by the ionic exchange reaction of $[H_2NMe_2]^+$ cation with rare earth ions, which is named as $RE^{3+} \subset [Y(DPA)_3]$ (RE = Eu, Tb, Sm, Dy) hybrid systems. The multi-color can be tuned for these functionalized hybrid systems and even white color luminescence can be integrated for $Sm^{3+} \subset [Y(DPA)_3]$. Besides, the fluorescent sensing property of $Tb^{3+} \subset [Y(DPA)_3]$ system is checked, which shows high selectivity towards Cr^{3+} with the concentration of 10^{-5} mol·L^{-1}.

Keywords Rare earth ion · Coordination polymer · Luminescence · Sensing · Ion exchange modification

Introduction

Luminescent rare earth ions have an unusual position in the fields of optical materials and devices for their remarking properties such as high color purity caused by their line-like emission, large Stokes shifts and wide lifetime range from microsecond to millisecond lifetimes [1–8]. But the 4f-4f transition of rare earth ion itself is spin-forbidden and can directly affect the efficiency of the luminescence output. Rare earth coordination compounds are ideal system to sensitize the luminescence of rare earth ions with so-called "antenna effect" [9–13]. Generally, the photophysical sensitization process involves the energy transfer from the triplet excited state of an organic ligand containing an antenna chromophore to the f-block ions [14, 15].

Rare earth coordination polymers with repeating coordination entities extending in 1, 2, or 3 dimensions, have attracted much attention for their potentials and advantages as inorganic–organic hybrid materials with infinite polymeric structure [16]. The variety of rare earth ions, organic linkers, and structural motifs affords an essentially infinite number of possible combinations [17–19]. These materials have shown their potential applications in luminescent thin film, biological imaging, and chemical sensors, etc. [20–25]. The luminescent properties of rare earth coordination compounds are very sensitive to their structural characteristics, coordination environment, and their interactions with guest species, which endows coordination compounds with inherent advantage in luminescent sensing [26–29]. Recently, these rare earth coordination compounds have unlimited potentials as chemical sensors, detecting cations, anions, small molecules, pH value and temperature [30–39].

Furthermore, rare earth coordination polymers are easily to realize the different rare earth ions substitution from each other for their similar physical properties [40–45]. This can develop a lot of rare earth hybrids based with coordination polymers, just like rare earth phosphors. On the other hand, there are a lot of metallic (including rare earth) coordination polymers with cationic dimethyl amino group ($H_2NMe_2^+$) in the DMF solution reaction systems [46–49]. So it can be expected to further introduce other rare earth ions through ionic exchange reaction with $H_2NMe_2^+$. For example, bio-MOF-1 ($Zn_8(ad)_4(BPDC)_6O{\cdot}2Me_2NH_2$, BPDC = biphenyl-4,4'-dicarboxylate, Ad = adeninate) has been proved to be functionalized with rare earth ions to show the characteristic

Electronic supplementary material The online version of this article (doi:10.1007/s10895-016-1847-7) contains supplementary material, which is available to authorized users.

✉ Bing Yan
byan@tongji.edu.cn

[1] Department of Chemistry, Tongji University, Siping Road 1239, Shanghai 200092, China

luminescence of them [50, 51]. We have also studied rare earth ions exchanged bio-MOF-1 and other coordination polymers, whose luminescence can be tuned and further applied to fluorescent sensing [52, 53]. Therefore, for these kinds of rare earth coordination polymers with $H_2NMe_2^+$, both ion substitution and ion exchange can be used to functionalize them to construct the functional hybrid systems.

Among rare earth ions, inert ions such as Y^{3+} are often used as matrices for traditional luminescent material, while other active ions such as Eu^{3+}, Tb^{3+}, Sm^{3+} and Dy^{3+} ions, act as vital activators. The synthesis of $[H_2NMe_2]_3[Eu(Tb)(DPA)_3]$ and rare earth ions doped $[H_2NMe_2]_3[RE(DPA)_3]$ systems through the ion substitution of framework rare earth ions have been reported [54–56]. Herein, different from the work, $[H_2NMe_2]_3[Y(DPA)_3]$ coordination polymer is synthesized and further functionalized to $RE^{3+} \subset [Y(DPA)_3]$ by ion exchange with rare earth ions considering the existence of $H_2NMe_2^+$. The multi-color luminescence of these coordination polymers are obtained and even the white emission is tuned. Moreover, $Tb^{3+} \subset [Y(DPA)_3]$ are selected to detect sensing properties.

Experimental Section

Materials and Instruments All the solvents and chemicals were available as A.R grade commercially. $RE(NO_3)_3 \cdot xH_2O$ (RE = Y, Eu, Tb, Sm, Dy) were prepared from their oxide by dissolving in nitric acid. Dimethylformamide (DMF) and 2,6-dipicolinic acid (2,6-H_2DPA) were used as received. The contents of RE^{3+} ions in the hybrids were determined with ICP-AES. The elemental analyses of C, H and N elements of the hybrids were measured with a CARIO-ERBA 1106 elemental analyzer. X-Ray powder diffraction patterns (XRD) were obtained Bruker Foucs D8 at 40 kV, 40 mA of Cu-Kα with a speed size of 0.02 and a scan speed of 0.10 s per step. We collected the data within 2θ range from 5 to 50°. A Nexus 912 AO446 infrared spectrum radiometer was used to measure Fourier transforms infrared spectra (FTIR) from 4000 to 400 cm^{-1}. The luminescence spectra were carried out by an Edinburgh FLS 920 phosphorimeter using a 450 W xenon lamp as excitation source. The luminescent lifetimes and quantum yields were also tested by the phosphorimeter. The spectra were corrected for variations in the output of the excitation source and for variations in the detector response. The quantum yield can be defined as the integrated intensity of the luminescence signal divided by the integrated intensity of the absorption signal. The absorption intensity was calculated by subtracting the integrated intensity of the light source with the sample in the integrating sphere from the integrated intensity of the light source with a blank sample in the integrating sphere.

Synthesis of $[H_2NMe_2]_3[Y(DPA)_3]$ (H_2DPA = 2,6-Dipicolinic Acid) The complex was obtained according to solvothermal method similar to ref. [54, 56]. 0.50 mmol $Y(NO_3)_3 \cdot xH_2O$ and 2 mmol H_2DPA were dissolved in a 50 mL of Teflon-lined stainless steel vessel, which was placed mixed solvent of 14 mL DMF and 2 mLH_2O previously. The mixture was hated to 120 °C and kept this temperature for 3 days. Then, cooling down to room temperature naturally, the products were collected after washing with DMF (5 × 3 mL) and drying under vacuum for 12 h. The contents of C, H, N and Y^{3+} were determined by elemental analysis, whose data are shown in Table S1.

Cation Exchanging Experiment $[H_2NMe_2]_3[Y(DPA)_3]$ (30 mg) was immersed in the 10 mL of DMF solutions of $RE(NO_3)_3 \cdot xH_2O$ and $M(NO_3)_x$ (RE^{3+} = Eu^{3+}, Tb^{3+}, Sm^{3+}, Dy^{3+}; M^{x+} = Na^+, Mg^{2+}, Al^{3+}, Cd^{2+}, Cr^{3+}, Co^{2+}, Fe^{2+}, Fe^{3+}, Ag^+, Cu^{2+}) with the concentration of 1 mmol/L for 3 days. We collected the PXRD after washing with DMF (5 × 3 mL) and drying under vacuum for 12 h. Among the cation exchange functionalized hybrid systems were named as $RE^{3+} \subset [Y(DPA)_3]$ (RE = Eu, Tb, Sm, Dy). The contents of C, H, N and RE^{3+} were determined by elemental analysis, whose data are shown in Table S1.

Luminescence Sensing Experiment $Tb^{3+} \subset [Y(DPA)_3]$ (10 mg) was simply immersed in the DMF solutions of $M(NO_3)_x$ with the concentration of 10^{-4} mol·L^{-1} and 10^{-5} mol·L^{-1} respectively at room temperature (M^{x+} = Na^+, Mg^{2+}, Al^{3+}, Cd^{2+}, Cr^{3+}, Co^{2+}, Fe^{2+}, Fe^{3+}, Ag^+, Cu^{2+}). The luminescent was then determined after vibrating under ultrasonic for 5 min.

Results and Discussion

Yttrium coordination polymer, $[H_2NMe_2]_3[Y(DPA)_3]$ ($[H_2NMe_2]^+$ = dimethyl amino cation; H_2DPA = 2,6-dipicolinic acid) is hydrothermally synthesized, whose scheme for the structure is shown in Fig. S1. Their crystal structures belong to a coordination sphere with N_3O_6 chromophore, whose coordination geometry can be described as a distorted tricapped trigonal prism consisting six carboxylato oxygen atoms and three pyridine nitrogen atoms. Among amine is more basic than the carboxylate group and so the protons are located on the dimethylamine molecules. The X-ray diffraction patterns of $[H_2NMe_2]_3[Y(DPA)_3]$ and rare earth ions exchanged hybrid systems $RE^{3+} \subset [Y(DPA)_3]$ are also checked and shown in Fig. 1, whose crystal diffractions are similar to unexchanged $[H_2NMe_2]_3[RE(DPA)_3]$ system. So the exchanged functionalization of $[H_2NMe_2]_3[Y(DPA)_3]$ cannot have influence on the crystal framework structure of $[Y(DPA)_3]^{3+}$.

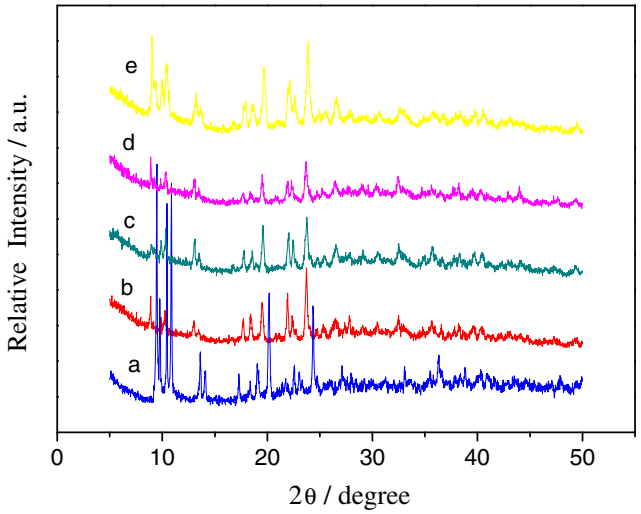

Fig. 1 PXRD patterns of $[H_2NMe_2]_3[Y(DPA)_3]$ (*a*) and $RE^{3+} \subset [Y(DPA)_3]$ (RE = Eu (*b*), Tb (*c*), Sm (*d*), Dy (*e*))

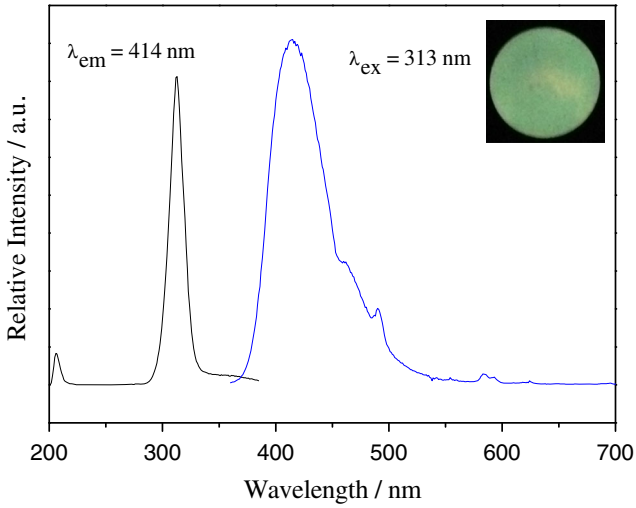

Fig. 2 The excitation and emission spectra of $[H_2NMe_2]_3[Y(DPA)_3]$ and the corresponding luminescent pictures under xenon lamp (*inset*)

The coordination interaction between rare earth ions and DPA can be shown from the selected FT-IR spectra analyses of $[H_2NMe_2]_3[Y(DPA)_3]$ (Fig. S2) and $Eu^{3+} \subset [Y(DPA)_3]$ (Fig. S3). The absorption band located at ~1619 cm^{-1} is assigned to the asymmetric stretching vibrations of C = O. Comparing with the free carboxyl groups whose absorption band of C = O is at ~1700 cm^{-1}, the lower wavenumber indicates the coordination between carboxyl groups and Y^{3+}.The peak located at ~ 1434 cm^{-1} can be assigned to the stretching vibration of C-C. The peak at ~1375 cm^{-1} may result from the amino C-N stretch. The absorption band at ~732 cm^{-1} can be ascribed to the C-H bending vibrations of the aromatic ring. All of these suggest similar coordination interactions between rare earth ions and DPA to construct the whole framework $[Y(DPA)_3]^{3-}$. In addition, three characteristic peaks of benzene ring stretching vibrations (1600 ~ 1500 cm^{-1}) remain after reaction. The asymmetric vibrations (1685 cm^{-1}) of carboxylate ions and its symmetric vibrations (1427 cm^{-1}) have changed simultaneously, proving the carboxyl groups have coordinated with rare earth ions [54, 55].

The emission and excitation spectra of these pure yttrium coordination polymer $[H_2NMe_2]_3[Y(DPA)_3]$ is measured and shown in Fig. 2. In the visible region, a number of very weak and narrow peaks (characteristic of the Laporte-forbidden f-f transitions of the Ln^{3+} ions) are observed. $[H_2NMe_2]_3[Y(DPA)_3]$ possess the emission of free DPA ligand exhibits excitation at 313 nm and emission at 414 nm which is presumably due to $\pi \rightarrow \pi^*$ electron transitions of pyridine cycle, while Y^{3+} ion only have little disturbance of the emission of DPA ligand for its coordination interaction.

After the ion exchange between rare earth ions with $H_2NMe_2^+$ ion to form $RE^{3+} \subset [Y(DPA)_3]$, different from $[H_2NMe_2]_3[Y(DPA)_3]$, the characteristic luminescence of rare earth ions (Eu^{3+}, Tb^{3+}, Sm^{3+}, Dy^{3+}) can be observed. This may be due to the energy transfer between $[Y(DPA)_3]^{3-}$ and RE^{3+} through the ionic interaction. Figure 3 shows the luminescent spectra of $Tb^{3+} \subset [Y(DPA)_3]$ and $Dy^{3+} \subset [Y(DPA)_3]$. For $Tb^{3+} \subset [Y(DPA)_3]$ hybrid systems in Fig. 3a, similar to $[H_2NMe_2]_3[Tb(DPA)_3]$, an apparent wide spectrum ranges in 250–400 nm, which has two excitation peaks. The excitation peaks to f-f transition of $Tb^{3+}$are too weak to be checked. The emission of $Tb^{3+} \subset [Y(DPA)_3]$ also shows the characteristic transitions ($^5D_4 \rightarrow {}^7F_J$, J = 6–3) of Tb^{3+} at 491, 545, 585, and 622 nm, respectively [57]. For $Dy^{3+} \subset [Y(DPA)_3]$ hybrids, it shows the excitation spectrum identical to $[Y(DPA)_3]$ and the weak f-f transition excitation of Dy^{3+} to the transition from $^6H_{15/2}$ to $^6P_{3/2}$ (325 nm), $^6P_{7/2}$ (351 nm), $^6P_{5/2}$ (365 nm), and $^4K_{17/2}$ (381 nm) [58]. The emission mainly displays two bands to Dy^{3+} characteristic transitions ($^4F_{9/2} \rightarrow {}^6H_J$, J = 15/2, 13/2) at 482, 573 nm (Fig. 3b). The inset pictures in the spectra show the color of these systems under xenon lamp. Under characteristic excitation of each material, various colours can be obtained such as blue-green for $Dy^{3+} \subset [Y(DPA)_3]$, and green for $Tb^{3+} \subset [Y(DPA)_3]$, respectively. Here $Tb^{3+} \subset [Y(DPA)_3]$ also exhibit the bright green luminescence due to the strong wide excitation band, while $Dy^{3+} \subset [Y(DPA)_3]$ possess the comparable intensity of both blue and yellow color to show the close white color emission.

Figure 4 displays the luminescent spectra of $Eu^{3+} \subset [Y(DPA)_3]$ and $Sm^{3+} \subset [Y(DPA)_3]$. Both of their excitation spectrum shows the similar feature to the excitation spectrum of $[H_2NMe_2]_3[Y(DPA)_3]$ with a wide band to the DPA ligands to form the charge transfer state Eu-O or Sm-O while no f-f transitions excitation of Sm^{3+} or Eu^{3+} can be checked. The emission spectra of $Eu^{3+} \subset [Y(DPA)_3]$ in Fig. 4a shows five narrow emission peaks at 580, 591, 614, 652 and 700 nm are observed and assigned to the characteristic $^5D_0 \rightarrow {}^7F_0$, $^5D_0 \rightarrow {}^7F_1$, $^5D_0 \rightarrow {}^7F_2$, $^5D_0 \rightarrow {}^7F_1$ and

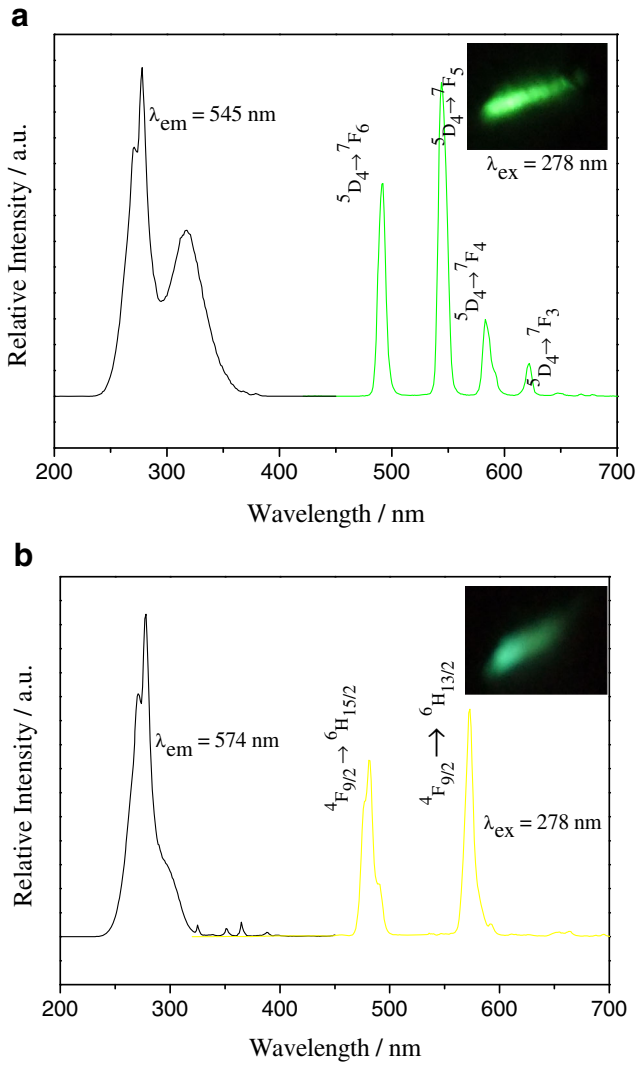

Fig. 3 The excitation and emission spectra of $RE^{3+} \subset [Y(DPA)_3]$ (RE = Tb (**a**), Dy (**b**)) and the corresponding luminescent pictures under xenon lamp

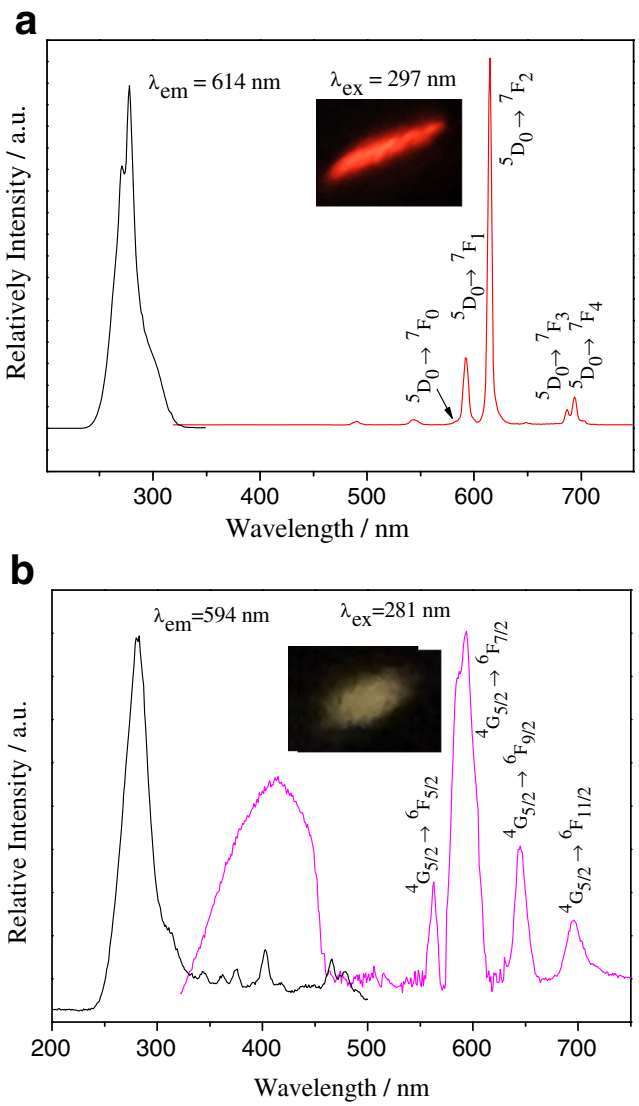

Fig. 4 The excitation and emission spectra of $RE^{3+} \subset [Y(DPA)_3]$(RE = Eu (**a**), Sm (**b**)) and the corresponding luminescent pictures under xenon lamp

$^5D_0 \rightarrow {}^7F_2$ transitions of Eu^{3+}, respectively [59]. And red luminescence is obtained (inset picture in Fig. 4a). The emission spectrum are originated from the characteristic transitions ($^4G_{5/2} \rightarrow {}^6H_J$, $J = 5/2, 7/2, 9/2, 11/2$) of Sm^{3+} at 561, 596, 644 and 703 nm, respectively (Fig. 4b) [58]. It is interesting that another wide emission band can be observed in the emission spectrum of the weak emission of Sm^{3+}, some disturbing peaks can be observed in the emission spectra of $Sm^{3+} \subset [Y(DPA)_3]$, corresponding to the $[Y(DPA)_3]^{3-}$.So it is predicted that the two emission bands may be integrate white-color luminescent output (see inset picture in Fig. 4b).

Moreover, considering the spectra with different luminescent region, some systems may be expected to realize to tune the close white luminescence. For samarium ion exchanged $Sm^{3+} \subset [Y(DPA)_3]$ hybrid system, both luminescence of $Sm^{3+} \subset [Y(DPA)_3]$ hybrid system, both luminescence of Sm^{3+} and $[Y(DPA)_3]^{3-}$ framework can be observed, resulting in the white color luminescence with CIE coordinates (0.3810, 0.2875). (See Fig. 5).

Furtherly, we determine the photoluminescent data of lifetimes and quantum yields of these hybrid systems, whose data are summarized in Table 1. Here it is worthy pointing out that they are all the data from the monitoring of rare earth ions' luminescence except for $[H_2NMe_2]_3[Y(DPA)_3]$ which is mainly due to the luminescence of DPA ligand coordinated to Y ions. It is interesting that the rare earth ions exchanged hybrid systems $RE^{3+} \subset [YDPA)_3]$ display the comparable value of lifetimes and quantum yields to pure coordination polymers $[H_2NMe_2]_3[RE(DPA)_3]$, which reveals that the ion exchanged functionalization of such rare earth coordination polymers is an effective approach to construct hybrid systems. So for rare earth coordination polymers with $[H_2NMe_2]^+$ ion, two kinds of strategies can be utilized to functionalize, ion

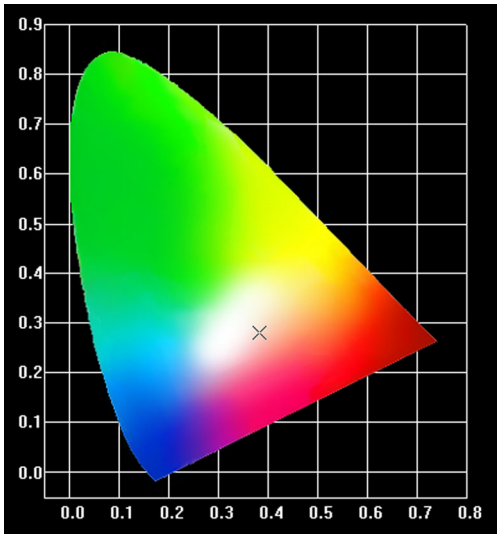

Fig. 5 CIE Chromaticity diagram of $Sm^{3+} \subset [Y(DPA)_3]$ when excited at 281 nm

substitution and ion exchange, both of which are benefit to realize the effective energy transfer and luminescence of photoactive rare earth ions [55, 56].

To examine and compare the sensing potential of $Tb^{3+} \subset [Y(DPA)_3]$ which is obtained through cation exchange, were suspended in DMF solutions containing different metal ions (Na^+, Ag^+, Mg^{2+}, Al^{3+}, Co^{2+}, Cr^{3+}, Cd^{2+}, Fe^{2+}, Fe^{3+}, Cu^{2+}) at the concentration of 10^{-4} mol·L^{-1} at first. The luminescent properties were recorded in Fig. S4 and Fig. S5, different with $[H_2NMe_2]_3[Tb(DPA)_3]$, $Tb^{3+} \subset [Y(DPA)_3]$ shows highly pronounced to Co^{2+}, Cr^{3+}, Fe^{3+} and Cu^{2+}, the selective sensing of Fe^{3+} is not as obvious as $[H_2NMe_2]_3[Tb(DPA)_3]$ [56]. The K_{SV} of these ions is displayed in Table S2. Subsequently, the concentration of metal solutions has been decreased to 10^{-5} mol·L^{-1} to explore the sensing properties of $Tb^{3+} \subset [Y(DPA)_3]$ furtherly. To our surprise, it shows high selectively towards Cr^{3+}, as is illustrated in Fig. 6, Further work is carried out to examine how the concentration of Cr^{3+} influences the luminescence of $Tb^{3+} \subset [Y(DPA)_3]$. As is exhibited in Fig. 7, the luminescent intensity of

Table 1 Luminescent data of $[H_2NMe_2]_3[RE(DPA)_3]$ and $RE^{3+} \subset [YDPA)_3]$

Materials	τ/μs	η/%
$[H_2NMe_2]_3[Y(DPA)_3]$	767	47
$Eu^{3+} \subset [Y(DPA)_3]$	1758	48
$Tb^{3+} \subset [Y(DPA)_3]$	1719	46
$Sm^{3+} \subset [Y(DPA)_3]$	463	13
$Dy^{3+} \subset [Y(DPA)_3]$	930	22

η Absolute luminescent quantum yields, η_{ET} energy transfer efficiencies from bio-MOF-1 (donor) to Ln^{3+} (acceptor)

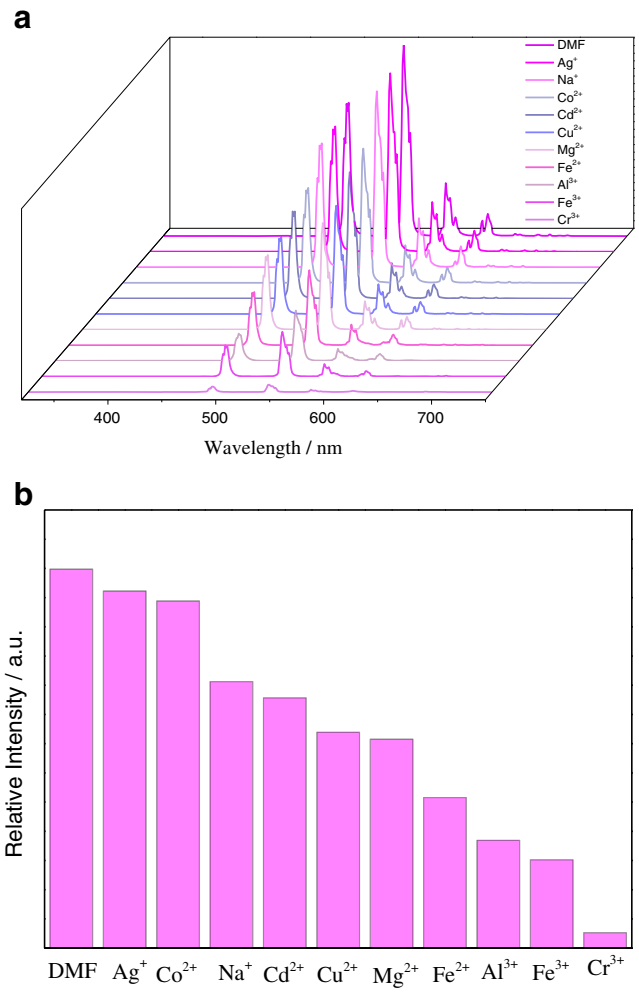

Fig. 6 **a** PL spectra of $Tb^{3+} \subset [Y(DPA)_3]$ interacting with different metal cations DMF solutions (10^{-5} mol/L) when excited at 278 nm; **b** The luminescent intensity of the $^5D_4 \rightarrow {}^7F_5$ transition of $Tb^{3+} \subset [Y(DPA)_3]$ interacting with different metal cations DMF solutions

$Tb^{3+} \subset [Y(DPA)]$ suspension decreased gradually as the concentration of Cr^{3+} varying from 0 to 100 μM. The Ksv value is calculated as 3.64×10^4, which reveals a strong quenching effect on the luminescence of $Tb^{3+} \subset [Y(DPA)_3]$. The quenching effects on luminescence of MOFs with the addition of metal ions may be attributed to the following factors: (i) interaction between the metal ions and organic ligands; (ii) collapse of the crystal structure; (iii) cation exchange between the central cations of coordination polymer and the targeted cations. PXRD was employed to study the structural data of original $[H_2NMe_2]_3[Tb(DPA)_3]$, $M^{z+} \subset [Tb(DPA)_3]$, $Tb^{3+} \subset [Y(DPA)_3]$, M^{z+},$Tb^{3+} \subset [Y(DPA)_3]$. For $M^{z+} \subset [Tb(DPA)_3]$, the quenching effect should originate from the less-effective transfer process of ligand to the central, which is due to the interaction between metal cations and organic ligands. For M^{z+}, $Tb^{3+} \subset [Y(DPA)_3]$, besides the less-effective transfer process of ligand to the central, the exchange between the Tb^{3+} and M^{z+} may also cause the

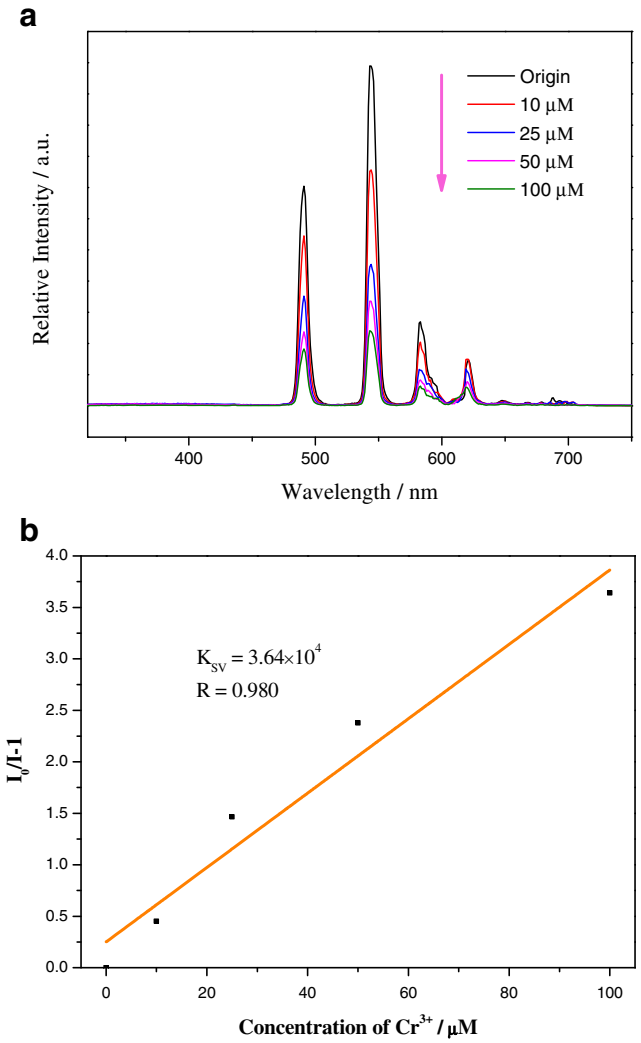

Fig. 7 **a** Emission spectra of $Tb^{3+} \subset [Y(DPA)_3]$ in various concentrations of Cr^{3+} when excited at 278 nm; **b** K_{SV} curve between I_0/I with the concentration of Cr^{3+}

quenching effect in a degree, which can lead to the decreasing selection of $Tb^{3+} \subset [Y(DPA)_3]$ to M^{z+}.

Conclusions

In summary, $[H_2NMe_2]_3[Y(DPA)_3]$ is prepared and further a novel strategy is used to modify $[H_2NMe_2]_3[Y(DPA)_3]$ through the ion exchange reaction between RE^{3+} and $[H_2NMe_2]^+$, resulting in hybrid systems $RE^{3+} \subset [Y(DPA)_3]$. It is interesting that the ion exchange functionalized hybrid systems possess the comparable luminescent lifetimes and quantum yields to the pure coordination polymers, revealing that it is an effective path to functionalize rare earth coordination polymers with $[H_2NMe_2]^+$ by means of ion exchange interaction. Furthermore, $Tb^{3+} \subset [Y(DPA)_3]$ is selected to explore their potential for sensing metal ions, which performs apparently selective and sensitive luminescence sensor for Cr^{3+} ion.

Acknowledgments This work is supported by the National Natural Science Foundation of China (21571142) and Developing Science Funds of Tongji University.

References

1. Ropp RC (2004) Luminescence and the solid state, 2 edn. Elsevier Science, Amsterdam
2. Kitai A (2008) Luminescent materials and applications. Wiley
3. Bunzli JCG, Piguet C (2005) Taking advantage of luminescent lanthanide ions. Chem Soc Rev 34:1048–1077
4. Montgomery CP, Murray BS, New EJ, Pal R, Parker D (2009) Cell-penetrating metal complex optical probes: targeted and responsive systems based on lanthanide luminescence. Acc Chem Res 42:925–937
5. Haas KL, Katherine J (2009) Application of metal coordination vhemistry yo rxplore and manipulate. Cell Biol Chem Rev 109: 4921–4960
6. de Bettencourt-Dias A (2007) Small molecule luminescent lanthanide ion complexes - photophysical characterization and recent developments. Curr Org Chem 11:1460–1480
7. Bunzli JCG (2010) Lanthanide luminescence for biomedical analyses and imaging. Chem Rev 110:2729–2755
8. Eliseeva SV, Bunzli JCG (2010) Lanthanide luminescence for functional materials and bio-sciences. Chem Soc Rev 39:189–227
9. Sabbatini N, Guardigli M, Lehn JM (1993) Luminescent lanthanide complexes as photochemical supramolecular devices. Coord Chem Rev 123:201–228
10. Justel T, Nikol H, Ronda C (1998) New developments in the field of luminescent materials for lighting and displays. Angew Chem Int Ed 37:3085–3103
11. Parker D, Dickins RS, Puschmann H, Crossl C, Howard JAK (2002) Being excited by lanthanide coordination complexes: aqua species, chirality, excited-state chemistry, and exchange dynamics. Chem Rev 102:1977–2010
12. Batten SR, Champness NR, Chen XM, Garcia-Martinez J, Kitagawa S, Ohrstrom L, O'Keeffe M, Suh MP, Reedijk J (2013) Terminology of metal–organic frameworks and coordination polymers. Pure Appl Chem 85:1715–1724
13. Novio F, Simmchen J, Vazquez-Mera N, Amorin-Ferre L, Ruiz-Molina D (2013) Coordination polymer nanoparticles in medicine. Coord Chem Rev 257:2839–2847
14. Binnemans K (2009) Lanthanide-based luminescent hybrid materials. Chem Rev 109:4283–4374
15. Regulacio MD, Pablico MH, Vasquez JA, Myers PN, Gentry S, Prushan M, Tam-Chang S, Stoll SL (2008) Luminescence of Ln(III) dithiocarbamate complexes (Ln = La, Pr, Sm, Eu, Gd, Tb, Dy). Inorg Chem 47:1512–1523
16. Huang YG, Jiang FL, Hong MC (2009) Magnetic lanthanide-transition-metal organic-inorganic hybrid materials: from discrete clusters to extended frameworks. Coord Chem Rev 253:2814–2834
17. Perry JJ IV, Perman JA, Zaworotko MJ (2009) Design and synthesis of metal-organic frameworks using metal-organic polyhedra as supermolecular building blocks. Chem Soc Rev 38:1400–1417
18. Zhao D, Timmons DJ, Yuan DQ, Zhou HC (2011) Tuning the topology and functionality of metal-organic frameworks by ligand design. Acc Chem Res 44:123–133
19. O'Keeffe M, Yaghi OM (2012) Deconstructing the crystal structures of metal-organic frameworks and related materials into their underlying nets. Chem Rev 112:675–702
20. Almeida Paz FA, Klinowski J, Vilela SMF, Tome JPC, Cavaleiro JAS, Rocha J (2012) Ligand design for functional metal-organic frameworks. Chem Soc Rev 41:1088–1110

21. Cui YJ, Chen BL, Qian GD (2014) Lanthanide metal-organic frameworks for luminescent sensing and light-emitting applications. Coord Chem Rev 273-274:76–86
22. Roy S, Chakraborty A, Maji TK (2014) Lanthanide–organic frameworks for gas storage and as magneto-luminescent materials. Coord Chem Rev 273-274:139–164
23. Zhang XJ, Wang WJ, Hu ZJ, Wang GN, Uvdal KS (2015) Coordination polymers for energy transfer: preparations, properties, sensing applications, and perspectives. Coord Chem Rev 284:206–235
24. Lu Y, Yan B (2014) Lanthanide organic-inorganic hybrids based on functionalized metal-organic frameworks (MOFs) for near-UV white LED. Chem Commun 50:15443–15446
25. Hao ZM, Song XZ, Zhu M, Meng X, Zhao SN, Su SQ, Yang WT, Song SY, Zhang HJ (2013) One-dimensional channel-structured Eu-MOF for sensing small organic molecules and Cu^{2+} ion. J Mater Chem A 1:11043–11050
26. Lu ZZ, Zhang R, Li YZ, Guo ZJ, Zheng HG (2011) Solvatochromic behavior of a nanotubular metal-organic framework for sensing small molecules. J Am Chem Soc 133:4172–4174
27. Lu Y, Yan B, Liu JL (2014) Nanoscale metal-organic framework as highly sensitive luminescent sensor for Fe^{2+} in aqueous solution and living cell. Chem Commun 50:9969–9972
28. Zhou JM, Shi W, Li HM, Li H, Cheng P (2014) Experimental studies and mechanism analysis of high-sensitivity luminescent sensing of pollutional small molecules and ions in Ln_4O_4 cluster based microporous metal-organic frameworks. J Phys Chem C 118: 416–426
29. Nadella S, Sahoo J, Subramanian PS, Sahu A, Mishra S, Albrecht M (2014) Sensing of phosphates by using luminescent Eu-III and Tb-III complexes: application to the microalgal cell *Chlorella vulgaris*. Chem Eur J 20:6047–6053
30. Lu Y, Yan B (2014) A ratiometric fluorescent pH sensor based on nanoscale metal-organic frameworks (MOFs) modified by europium (III) complex. Chem Commun 50:13323–61332
31. Harbuzaru BV, Corma A, Rey F, Jorda JL, Ananias D, Carlos LD, Rocha J (2009) A miniaturized linear pH sensor based on a highly photoluminescent self-assembled europium(III) metal-organic framework. Angew Chem Int Ed 48:6476–6479
32. Zhou Y, Yan B, Lei F (2014) Postsynthetic lanthanides functionalization of nanosized metal-organic frameworks for highly sensitive ratiometric luminescent nanothermometers. Chem Commun 50:15235–15238
33. Gao CJ, Kirillov AM, Dou W, Tang XL, Liu LL, Yan XH, Xie YJ, Zang PX, Liu WS, Tang Y (2014) Self-assembly synthesis, structural features, and photophysical properties of dilanthanide domplexes derived from a novel amide type ligand: energy transfer from Tb(III) to Eu(III) in a heterodinuclear derivative. Inorg Chem 53:935–942
34. Rao XT, Song T, Gao JK, Cui YJ, Yang Y, Wu CD, Chen BL, Qian GD (2013) A highly sensitive mixed lanthanide metal-organic framework self-calibrated luminescent thermometer. J Am Chem Soc 135:15559–15564
35. Cui YJ, Xu H, Yue YF, Guo ZY, Yu JC, Chen ZX, Gao JK, Yang Y, Qian GD, Chen BL (2012) A luminescent mixed-lanthanide metal-organic framework thermometer. J Am Chem Soc 134:3979–3982
36. Zhou Y, Chen HH, Yan B (2014) Eu^{3+} post-functionalized nanosized metal-organic framework for cation exchange-based Fe^{3+}–sensing in aqueous environment. J Mater Chem A 2:13691–13697
37. Zhou Y, Yan B (2015) Lanthanides post-functionalized nanocrystalline metal-organic frameworks for tunable white-light emission and orthogonal multi-readout thermometry". Nanoscale 7:4063–4069
38. Zhou XH, Li L, Li HH, Li A, Yang T, Huang W (2013) A flexible Eu(III)-based metal-organic framework: turn-off luminescent sensor for the detection of Fe(III) and picric acid. Dalton Trans 42:12403–12409
39. Hao JN, Yan B (2015) A water-stable lanthanide-functionalized MOF as a highly selective and sensitive fluorescent probe for Cd^{2+}. Chem Commun 51:7737–7740
40. Kerbellec N, Kustaryono D, Haquin V, Etienne M, Daiguebonne C, Guillou O (2009) An unprecedented family of lanthanide-containing coordination polymers with highly tunable emission properties. Inorg Chem 48:2837–2843
41. de Melo EF, Santana NC, Bezerra Alves KG, de Sá GF, de Melo CP, Rodrigues MO, Júnior SA (2013) LnMOF@PVA nanofiber: energy transfer and multicolor light-emitting devices. J Mater Chem C 1: 7574–7581
42. Zhang HB, Shan XC, Ma ZJ, Zhou LJ, Zhang MJ, Lin P, Hu SM, Ma E, Li RF, Guo XG, Du SW (2014) A highly luminescent chameleon: fine-tuned emission trajectory and controllable energy transfer. J Mater Chem C 2:1367–1371
43. He YP, Tan YX, Zhang J (2014) Guest inducing fluorescence switching in lanthanide-tris((4-carboxyl)phenylduryl)amine frameworks integrating porosity and flexibility. J Mater Chem C 2:4436–4441
44. Duan TW, Yan B (2014) Hybrids based on lanthanide ions activated yttrium metal organic frameworks: functional assembly, polymer film preparation and luminescence tuning. J Mater Chem C 2: 5098–5104
45. Hao JN, Yan B (2014) Amino-decorated lanthanide (III) – organic extended frameworks for multi-color luminescence and fluorescence sensing. J Mater Chem C 2:6758–6764
46. Sun LB, Xing HZ, Liang ZQ, Yu JH, Xu RR (2013) A 4 + 4 strategy for synthesis of zeolitic metal-organic frameworks: an indium-MOF with SOD topology as a light-harvesting antenna. Chem Commun 49:11155–11157
47. Gai YL, Jiang FL, Chen L, Bu Y, Su KZ, Thabaiti AA, Hong MC (2013) Photophysical studies of europium coordination polymers based on a tetracarboxylate ligand. Inorg Chem 52:7658–7665
48. Chen Z, Sun YW, Zhang LL, Sun D, Liu FL, Meng QG, Wang RM, Sun DF (2013) A tubular europium-organic framework exhibiting selective sensing of Fe^{3+} and Al^{3+} over mixed metal ions. Chem Commun 49:11557–11559
49. Ma ML, Ji C, Zang SQ (2013) Syntheses, structures, tunable emission and white light emitting Eu^{3+} and Tb^{3+} doped lanthanide metal-organic framework materials. Dalton Trans 42: 10579–10586
50. An JY, Geib SJ, Rosi NL (2009) Cation-triggered drug release from a porous zinc-adeninate metal–organic framework. J Am Chem Soc 131:8376–8377
51. An JY, Shade CM, Chengelis-Czegan DA, Petoud S, Rosi NL (2011) Zinc-adeninate metal-organic framework for aqueous encapsulation and sensitization of near-infrared and visible emitting lanthanide cations. J Am Chem Soc 133:1220–1223
52. Shen X, Yan B (2015) Polymer hybrid thin films based on rare earth ion-functionalized MOF: photoluminescence tuning and sensing as thermometer. Dalton Trans 44:1875–1881
53. Shen X, Yan B (2015) Photofunctional hybrids of lanthanide functionalized bio-MOF-1 for fluorescence tuning and sensing. J Colloid Interface Sci 451:63–68
54. Mooibroek TJ, Gamez P, Pevec A, Kasunic M, Kozlevcar B, Fu WT, Reedijk J (2007) Efficient, stable, tunable, and easy to synthesize, handle and recycle luminescent materials: $[H_2NMe_2]_3[Ln(III)(2,6\text{-dipicolinolate})_3]$ (Ln = Eu, Tb, or its solid solutions). Dalton Trans 39:6483–6487
55. Zhang HB, Shan XC, Zhou LJ, Lin P, Li RF, Ma E, Guo XG, Du SW (2013) Full-color fluorescent materials based on mixed-lanthanide(III) metal–organic complexes with high-efficiency white light emission. J Mater Chem C 1:888–891

56. Weng H, Yan B (2016) Lanthanide coordination polymers for multi-color luminescence and sensing of Fe^{3+}. Inorg Chem Commun 63:11–15
57. Carnall WT, Fields PR, Rajnak K (1968) Electronic energy levels of the trivalent lanthanide aquo ions. III. Tb^{3+}. J Chem Phys 49:4447–4449
58. Carnall WT, Fields PR, Rajnak K (1968) Electronic energy levels in the trivalent lanthanide aquo ions. I. Pr^{3+}, Nd^{3+}, Pm^{3+}, Sm^{3+}, Dy^{3+}, Ho^{3+}, Er^{3+}, and Tm^{3+}. J Chem Phys 49:4424–4442
59. Carnall WT, Fields PR, Rajnak K (1968) Electronic energy levels of the trivalent lanthanide aquo ions. IV. Eu^{3+}. J Chem Phys 49:4450–4455